別添Figure. 4 LPS処理による肝臓中グルタチオンの低下

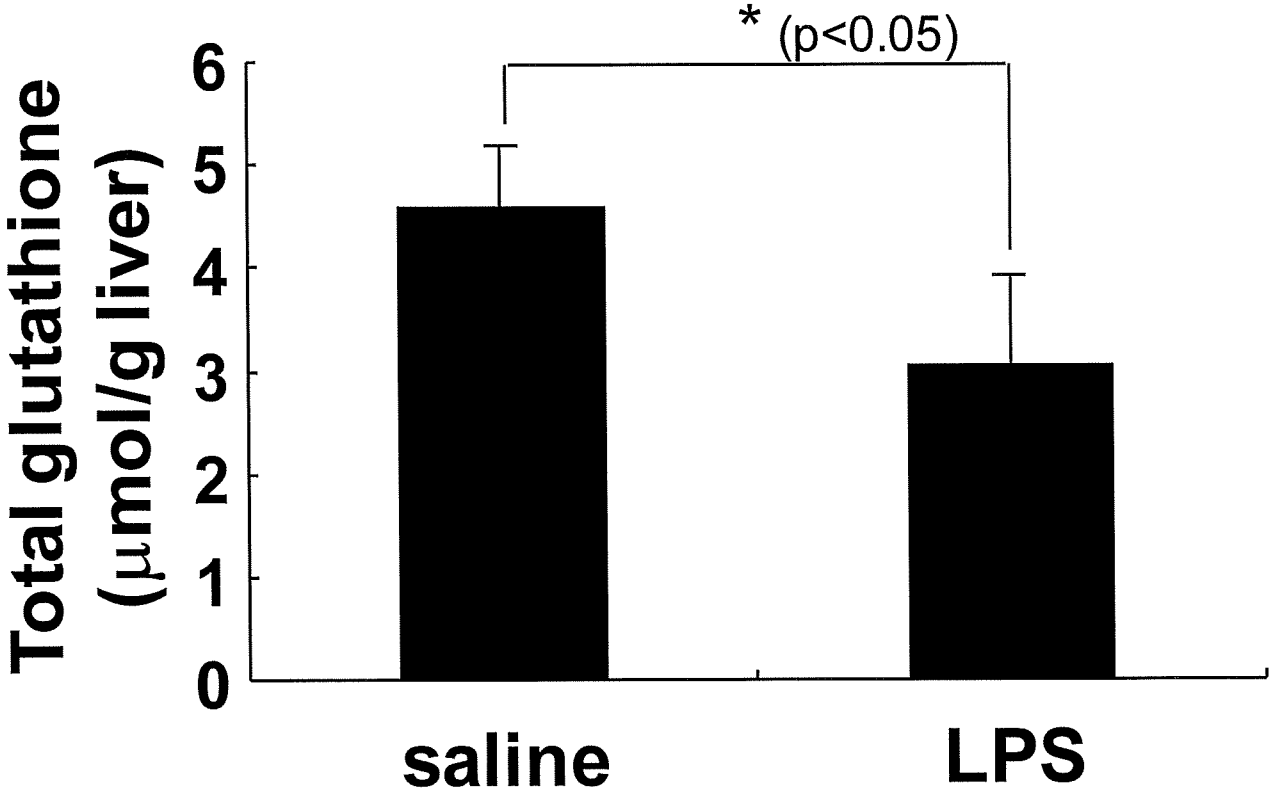

LPS(1mg/kg, i.p.)投与2時間後に肝臓を回収・調製し、Dithiobisnitrobenzoic acid (DTNB)を用いた酵素サイクル法によりグルタチオン濃度を測定。

別添Figure. 5 GSH/NAC投与による肝障害の抑制

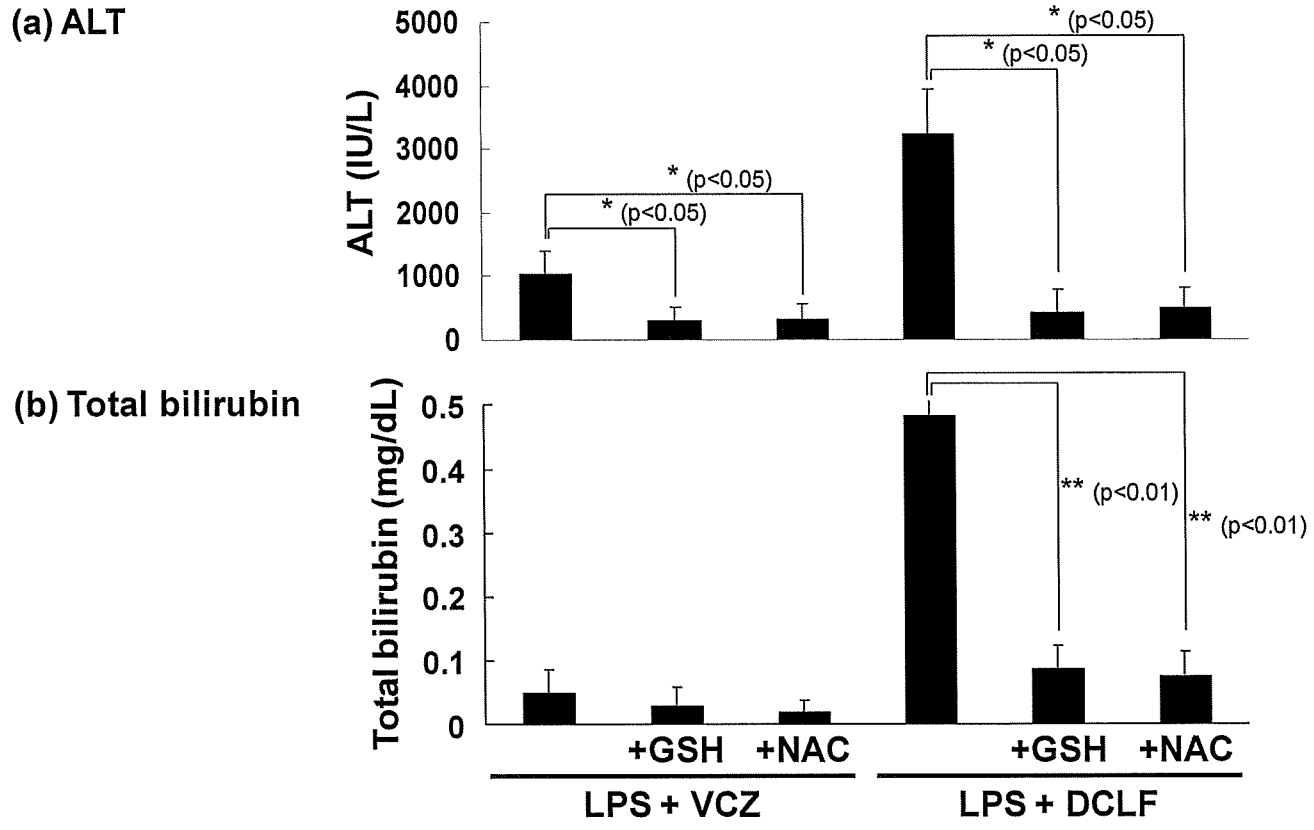

LPS投与1時間前より、GSH(100mg/kg, s.c.)もしくはNAC(100mg/kg, s.c.)を投与し、薬物投与12時間後に血清を回収し、(a)ALT、(b)総ビリルビンを測定。

別添Figure. 6 グルタチオン枯渇による肝障害の誘発

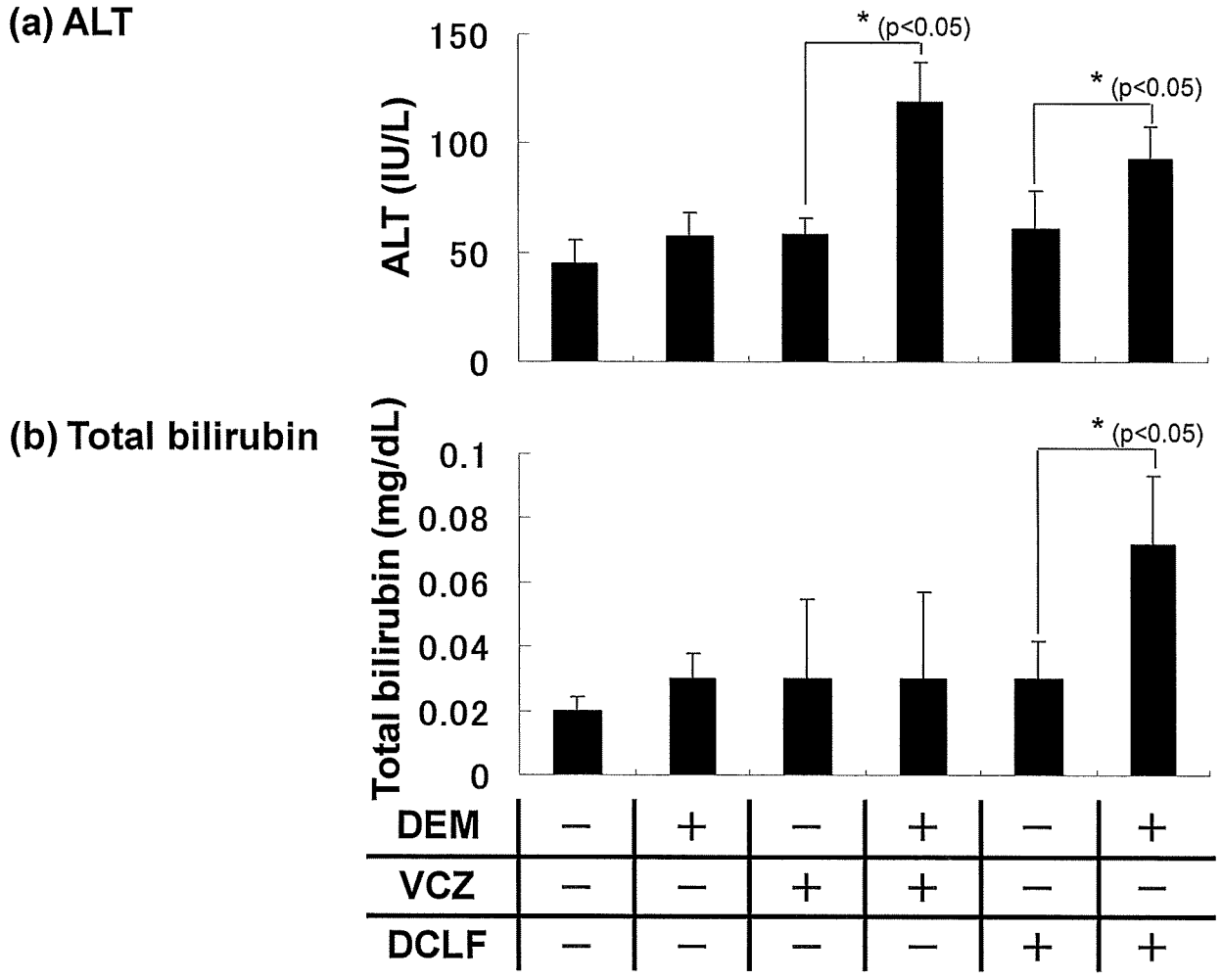

DEM(3mmol/kg, i.p.)投与2時間後にVCZ(30mg/kg, i.v.)もしくはDCLF(100mg/kg, i.v.)を投与。
薬物投与12時間後に血清を回収し、(a)ALT、(b)総ビリルビンを測定。

別添Figure.7 サイトカイン阻害による肝障害の抑制

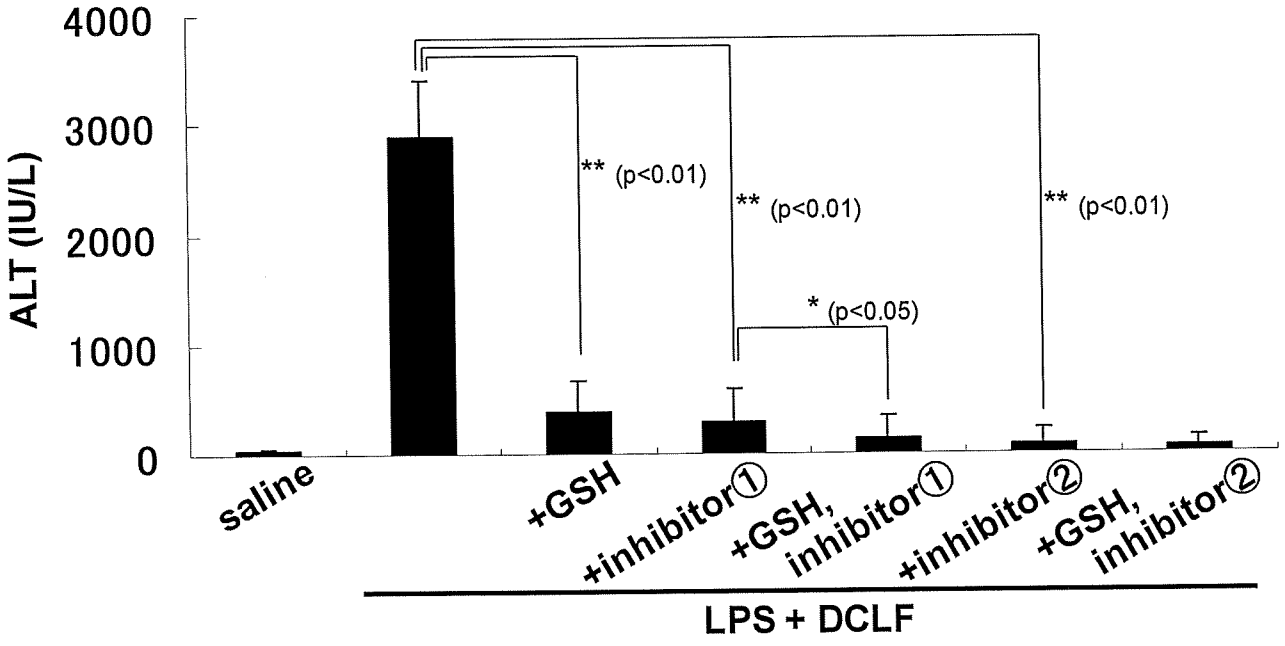

LPS投与1時間前より、GSH(100mg/kg, s.c.)もしくはサイトカインに対する阻害剤(inhibitor ①,②)を投与し、薬物投与12時間後に血清中ALTを測定。

別添４

研究成果の刊行に関する一覧表

雑誌

発表者氏名	論文タイトル名	発表誌名	巻号	ページ	出版年
Soga, T.,* Igarashi, K., Itoh, C., Mizobuchi, K., Zimmermann, H., Tomita, M.,	”Metabolomic Profiling of Anionic Metabolites by Capillary Electrophoresis Mass Spectrometry”	***Anal. Chem.***	**81**,	6165-6174,	2009
曽我朋義	メタボロミクス－網羅的代謝物質解析の医学・医療へのあらたな応用	医学のあゆみ	Vol231, Nos.12,13	1143	2009
平山明由、曽我朋義	ヒト癌組織のメタボローム解析	医学のあゆみ	Vol231, Nos.12,13	1145-1149	2009
曽我朋義	メタボローム測定装置の発明,	発明 The Invention	Vol106 (11)	29-31,	2009

Anal. Chem. 2009, *81*, 6165–6174

Metabolomic Profiling of Anionic Metabolites by Capillary Electrophoresis Mass Spectrometry

Tomoyoshi Soga,*,† Kaori Igarashi,† Chiharu Ito,† Katsuo Mizobuchi,‡ Hans-Peter Zimmermann,§ and Masaru Tomita†

Institute for Advanced Biosciences, Keio University, Tsuruoka, Yamagata 997-0052, Japan, Agilent Technologies, 9-1 Takakura-cho, Hachioji, Tokyo 192-8510, Japan, and Agilent Technologies, Hewlett-Packard-Strasse 8, 76337 Waldbronn, Germany

We describe a sheath flow capillary electrophoresis time-of-flight mass spectrometry (CE-TOFMS) method in the negative mode using a platinum electrospray ionization (ESI) spray needle, which allows the comprehensive analysis of anionic metabolites. The material of the spray needle had significant effect on the measurement of anions. A stainless steel spray needle was oxidized and corroded at the anodic electrode due to electrolysis. The precipitation of iron oxides (rust) plugged the capillary outlet, resulting in shortened capillary lifetime. Many anionic metabolites also formed complexes with the iron oxides or migrating nickel ion, which was also generated by electrolysis and moved toward the cathode (the capillary inlet). The metal−anion complex formation significantly reduced detection sensitivity of the anionic compounds. The use of a platinum ESI needle prevented both oxidation of the metals and needle corrosion. Sensitivity using the platinum needle increased from several- to 63-fold, with the largest improvements for anions exhibiting high metal chelating properties such as carboxylic acids, nucleotides, and coenzyme A compounds. The detection limits for most anions were between 0.03 and 0.87 μmol/L (0.8 and 24 fmol) at a signal-to-noise ratio of 3. This method is quantitative, sensitive, and robust, and its utility was demonstrated by the analysis of the metabolites in the central metabolic pathways extracted from mouse liver.

Metabolism is the entire network of chemical reactions that occur in a cell in order to maintain life, in which one metabolite is transformed into another by a sequence of enzymes. Among the whole cellular metabolic network, central carbon metabolism, composed of glycolysis, the pentose phosphate pathway, and the tricarboxylic acid (TCA) cycle, plays key functions in substrate degradation, energy and cofactor regeneration, and biosynthetical precursor supply (DNA, RNA, proteins, peptideglycan, and lipid bilayers).[1,2] Interestingly, all the components involved in the central carbon and energy metabolism are negatively charged: phosphorylated saccharides, phosphorylated carboxylic acids, carboxylic acids, coenzyme A (CoA) compounds, nucleotides, and nicotinamide adenine dinucleotides.

As the importance of metabolomics is recognized, several large-scale metabolite analysis methods using GC/MS,[3] LC/MS,[2,4,5] NMR[6−8] or Fourier transform ion cyclotron resonance mass spectrometry (FTICR-MS)[9,10] have been developed. However, only a limited number of methodologies enable the simultaneous analysis of the anionic metabolites due to their extremely large physicochemical diversity.

Recently, approaches based on capillary electrophoresis mass spectrometry (CE-MS)[11,12] and CE time-of-flight mass spectrometry (CE-TOFMS)[13] have emerged as powerful tools for the comprehensive analysis of charged metabolites and have played a critical role in understanding intricate biochemical and biological systems.[13−19]

* To whom correspondence should be addressed. Phone: (+81) 235 29 0528. Fax: (+81) 235 29 0574. E-mail: soga@sfc.keio.ac.jp.
† Keio University.
‡ Agilent Technologies, Japan.
§ Agilent Technologies, Germany.

10.1021/ac900675k CCC: $40.75
Published on Web 06/12/2009

(1) Sonenshein, A. L. *Nat. Rev. Microbiol.* 2007, *5*, 917–927.
(2) Yang, W. C.; Sedlak, M.; Regnier, F. E.; Mosier, N.; Ho, N.; Adamec, *J. Anal. Chem.* 2008, *80*, 9508–9516.
(3) Fiehn, O.; Kopka, J.; Dormann, P.; Altmann, T.; Trethewey, R. N.; Willmitzer, L. *Nat. Biotechnol.* 2000, *18*, 1157–1161.
(4) Plumb, R.; Granger, J.; Stumpf, C.; Wilson, I. D.; Evans, J. A.; Lenz, E. M. *Analyst* 2003, *128*, 819–823.
(5) Yoshida, H.; Mizukoshi, T.; Hirayama, K.; Miyano, H. *J. Agric. Food Chem.* 2007, *55*, 551–560.
(6) Reo, N. V. *Drug Chem. Toxicol.* 2002, *25*, 375–382.
(7) Coen, M.; Lenz, E. M.; Nicholson, J. K.; Wilson, I. D.; Pognan, F.; Lindon, J. C. *Chem. Res. Toxicol.* 2003, *16*, 295–303.
(8) Coen, M.; Ruepp, S. U.; Lindon, J. C.; Nicholson, J. K.; Pognan, F.; Lenz, E. M.; Wilson, I. D. *J. Pharm. Biomed. Anal.* 2004, *35*, 93–105.
(9) Aharoni, A.; Ric de Vos, C. H.; Verhoeven, H. A.; Maliepaard, C. A.; Kruppa, G.; Bino, R.; Goodenowe, D. B. *Omics* 2002, *6*, 217–234.
(10) Hirai, M. Y.; Yano, M.; Goodenowe, D. B.; Kanaya, S.; Kimura, T.; Awazuhara, M.; Arita, M.; Fujiwara, T.; Saito, K. *Proc. Natl. Acad. Sci. U.S.A.* 2004, *101*, 10205–10210.
(11) Soga, T.; Ohashi, Y.; Ueno, Y.; Naraoka, H.; Tomita, M.; Nishioka, T. *J. Proteome Res.* 2003, *2*, 488–494.
(12) Edwards, J. L.; Chisolm, C. N.; Shackman, J. G.; Kennedy, R. T. *J. Chromatogr., A* 2006, *1106*, 80–88.
(13) Soga, T.; Baran, R.; Suematsu, M.; Ueno, Y.; Ikeda, S.; Sakurakawa, T.; Kakazu, Y.; Ishikawa, T.; Robert, M.; Nishioka, T.; Tomita, M. *J. Biol. Chem.* 2006, *281*, 16768–16776.
(14) Ishii, N.; Nakahigashi, K.; Baba, T.; Robert, M.; Soga, T.; Kanai, A.; Hirasawa, T.; Naba, M.; Hirai, K.; Hoque, A.; Ho, P. Y.; Kakazu, Y.; Sugawara, K.; Igarashi, S.; Harada, S.; Masuda, T.; Sugiyama, N.; Togashi, T.; Hasegawa, M.; Takai, Y.; Yugi, K.; Arakawa, K.; Iwata, N.; Toya, Y.; Nakayama, Y.; Nishioka, T.; Shimizu, K.; Mori, H.; Tomita, M. *Science* 2007, *316*, 593–597.
(15) Ohashi, Y.; Hirayama, A.; Ishikawa, T.; Nakamura, S.; Shimizu, K.; Ueno, Y.; Tomita, M.; Soga, T. *Mol. Biosyst.* 2008, *4*, 135–147.
(16) Yoshida, S.; Imoto, J.; Minato, T.; Oouchi, R.; Sugihara, M.; Imai, T.; Ishiguro, T.; Mizutani, S.; Tomita, M.; Soga, T.; Yoshimoto, H. *Appl. Environ. Microbiol.* 2008, *74*, 2787–2796.

Application of the sheath flow CE-MS to the analysis of anionic metabolites has been successfully performed using the "negative mode" and a cationic polymer coated capillary.[20] This methodology reverses electroosmotic flow (EOF)[21] toward the anode (the MS direction) to prevent a deleterious current drop. The method enabled the large-scale determination of anionic metabolites, however, with limitations. Several anionic metabolites such as citrate, nucleotides, and CoA compounds were not detected or were detected as poorly shaped peaks.[20,22,23] To overcome the problem, a pressure-assisted CE-MS method[24] was used for these analytes.[22,23] While successful, two separate CE-MS methods for anions were necessary,[11] and moreover, these approaches were not ideal. Additionally, the capillaries frequently clogged.

Recently, it was found that these problems were caused by metal ions generated from the stainless steel needle of the electrospray ionization (ESI) sprayer. Iron oxides formed at the capillary outlet, while nickel ions migrated into the separation capillary and formed complexes with many anions. Here, we propose an improved sheath flow CE-MS method for the analysis of anionic metabolites using a platinum ESI spray needle. The platinum material has a low ionization tendency and does not generate metal ions through electrolysis. This approach overcame the problems and provided robust and sensitive analysis of most of the anionic metabolites and was successfully applied to the quantitative analysis of mouse hepatic metabolites in the central carbon and energy metabolic pathways.

EXPERIMENTAL SECTION

Chemicals. Glycerophosphate was purchased from Nacalai Tesque (Kyoto, Japan), 2-morpholinoethanesulfonate (MES, internal standard) from Dojindo (Kumamoto, Japan), and hexakis-(2,2-difluorothoxy)-phosphazene (Hexakis) from SynQuest Laboratories (Alachua, FL). All other reagents were obtained from Sigma-Aldrich (St. Louis, MO) or Wako (Osaka, Japan). Individual stock solutions of carboxylic acids, phosphorylated saccharides, and phosphorylated carboxylic acids were prepared at a concentration of 100 mM, and stock solutions for other compounds of 10 mM were prepared in Milli-Q water, except for fumarate and trimesate (reference peak) which were prepared in 0.1 M NaOH and succinyl CoA which was prepared in 0.1 M HCl. The working mixture standard was prepared by diluting these stock solutions with Milli-Q water just before injection. All chemicals were of analytical or reagent grade. Water was purified with a Milli-Q purification system (Millipore, Bedford, MA).

Metabolite Extraction. Liver tissue (approximately 300 mg) was immediately plunged into methanol (1 mL) containing 300 μM each of L-methionine sulfone and 2-morpholinoethanesulfonate (MES) (internal standards) and homogenized for 2 min to inactivate enzymes. Then Milli-Q water (500 μL) was added, 300 μL of the solution was transferred, and 200 μL of chloroform was added and mixed well. The solution was centrifuged at 15 000 rpm for 15 min at 4 °C, and the separated 200 μL aqueous layer was centrifugally filtered through a Millipore 5 kDa cutoff filter to remove proteins. The filtrate (100 μL) was lyophilized and dissolved in 50 μL of Milli-Q water containing reference compounds (200 μM each of trimesate and 3-aminopyrrolidine). The solution (2 μM) was diluted with 18 μL of Milli-Q water and then injected into the CE-TOFMS system.[13]

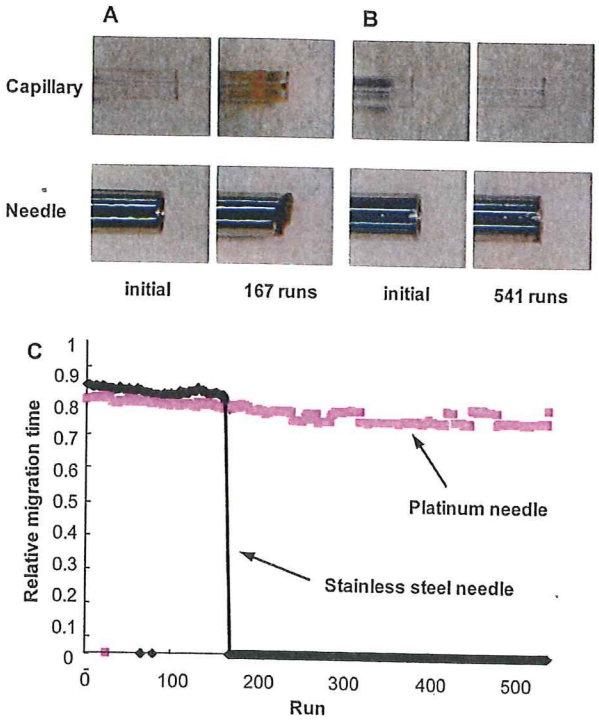

Figure 1. Robustness of the CE-TOFMS system in the anion standard analysis. Photograph of the capillary outlet and the tip of the needle of the COSMO(+) capillary obtained by the CE-ESI-MS sprayer with (A) the SST316Ti stainless steel needle and (B) the platinum needle. (C) Endurance of the system between the SST316Ti stainless steel needle (black) and platinum needle (magenta). The endurance was expressed using the relative migration time of lactate, which was calculated by normalization with the migration time of MES (internal standard). Experimental conditions are described in the Experimental Section.

Instrumentation. All CE-ESI-MS experiments were performed using an Agilent CE capillary electrophoresis system, an Agilent G3250AA LC/MSD TOF system, an Agilent1100 series isocratic HPLC pump, a G1603A Agilent CE-MS adapter kit, and a G1607A Agilent CE-ESI-MS sprayer kit (Agilent Technologies, Waldbronn, Germany). The CE-MS adapter kit includes a capillary cassette which facilitates thermostating of the capillary, and the CE-ESI-MS sprayer kit which simplifies coupling the CE system with MS systems was equipped with an electrospray source. For system control and data acquisition, we used G2201AA Agilent ChemStation software for CE and Agilent TOF (Analyst QS) software for TOFMS.

In addition, the original Agilent SST316Ti stainless steel (Fe/Cr/Ni/Mo/Ti; 68:18:11:2:1) ESI needle was replaced with passivated SST316Ti stainless steel (with 1% formic acid and 20%

(17) Sato, S.; Soga, T.; Nishioka, T.; Tomita, M. *Plant J.* **2004**, *40*, 151–163.
(18) Kinoshita, A.; Tsukada, K.; Soga, T.; Hishiki, T.; Ueno, Y.; Nakayama, Y.; Tomita, M.; Suematsu, M. *J. Biol. Chem.* **2007**, *282*, 10731–10741.
(19) Williams, B. J.; Cameron, C. J.; Workman, R.; Broeckling, C. D.; Sumner, L. W.; Smith, J. T. *Electrophoresis* **2007**, *28*, 1371–1379.
(20) Soga, T.; Ueno, Y.; Naraoka, H.; Ohashi, Y.; Tomita, M.; Nishioka, T. *Anal. Chem.* **2002**, *74*, 2233–2239.
(21) Lukacs, K. D.; Jorgenson, J. W. *J. High Resolut. Chromatogr. Chromatogr. Commun.* **1985**, *8*, 407–411.
(22) Soga, T.; Ueno, Y.; Naraoka, H.; Matsuda, K.; Tomita, M.; Nishioka, T. *Anal. Chem.* **2002**, *74*, 6224–6229.
(23) Soga, T.; Ishikawa, T.; Igarashi, S.; Sugawara, K.; Kakazu, Y.; Tomita, M. *J. Chromatogr., A* **2007**, *1159*, 125–133.
(24) Cao, P.; Moini, M. *Electrophoresis* **1998**, *19*, 2200–2206.

Table 1. Reproducibility, Linearity, and Sensitivity

compound	RSD (n = 8) (%) migration time	RSD (n = 8) (%) peak area	linearity correlation	detection limit (μmol/L)	improved sensitivity ratio[a]
glyoxylate	0.6	11.1	0.997	8.0	0.9
glycolate	0.6	12.4	0.997	5.2	1.7
pyruvate	0.5	8.8	0.999	9.5	0.8
lactate	0.6	5.7	0.985	2.9	1.1
fumarate	0.5	9.4	0.989	0.32	1.4
succinate	0.5	6.3	0.999	0.23	1.6
malate	0.5	4.5	0.994	0.14	4.5
2-oxoglutarate	0.5	5.3	0.985	0.73	4.9
cysteine sulfinate	0.6	6.5	0.998	0.36	4.0
PEP	0.5	5.2	0.995	0.12	3.0
DHAP	0.6	7.8	0.998	0.40	2.2
glycerophosphate	0.6	8.9	0.999	0.46	1.2
cis-aconitate	0.5	7.2	0.997	0.12	4.4
3-phosphoglycerate	0.5	4.9	0.995	0.19	2.8
isocitrate	0.5	3.6	0.996	0.19	6.0
citrate	0.5	7.3	0.988	0.09	63
gluconate	0.7	5.1	0.999	1.1	0.8
E4P	0.6	6.0	0.999	0.81	2.1
Ru5P	0.6	2.7	0.999	0.21	2.4
R5P	0.6	5.1	0.999	0.26	1.9
G1P	0.6	2.1	0.983	0.15	1.9
F6P	0.6	3.5	0.980	0.19	3.4
G6P	0.6	2.4	0.992	0.16	1.6
2,3DPG	0.5	5.8	0.997	0.13	35
6-phosphogluconate	0.5	5.4	0.999	0.18	2.9
F1,6P	0.5	5.4	0.999	0.17	3.1
AMP	0.7	3.5	0.999	0.11	2.1
IMP	0.7	4.8	0.999	0.11	2.9
GMP	0.7	3.6	0.999	0.09	2.0
NADPH[b]	0.6	4.3	0.990	0.45	2.7
CoA[b]	0.6	6.1	0.994	0.03	nc[c]
acetyl CoA[b]	0.6	5.2	0.999	0.04	5.2
malonyl CoA[b]	0.6	6.6	0.995	0.05	7.6
ADP	0.6	3.9	0.995	0.06	5.3
succinyl CoA[b]	0.6	12.1	0.996	0.15	10
GDP	0.6	5.6	0.996	0.11	5.5
UTP	0.6	3.4	0.999	0.10	7.8
ATP	0.6	5.8	0.999	0.22	6.6
GTP	0.6	14.4	0.989	0.10	15
NAD	1.1	4.8	0.999	0.11	1.8
NADH	0.7	3.4	0.999	0.49	11
NADP	0.7	6.1	0.999	0.10	2.4
FAD	0.8	10.5	0.999	0.12	2.8

[a] Improved sensitivity was calculated by dividing the detection limit with the SST316Ti stainless steel by that with the platinum needle. [b] Detected at the divalent $[M - 2H]^{2-}$ ion. [c] nc, not calculated. Improved sensitivity of CoA was not calculated because CoA was not determined by the SST316Ti stainless steel.

isopropanol aqueous solution at 80 °C for 30 min) and platinum. Metal amounts in run buffer solution in the inlet vial and separation capillary were determined using an Agilent 7500 inductivity coupled plasma mass spectrometer (Tokyo, Japan). For the capillary analysis, the polyimide coating was burned with a lighter and removed with methanol, and then the capillary was cut into five pieces (each 20 cm). Each capillary (5.4 mg) was dissolved by ultrasonic treatment in 8 mL of 38% hydrofluoric acid for 80 min, and this solution was used for the inductivity coupled plasma mass spectrometry (ICP-MS) analysis.

CE-TOFMS Conditions for Anionic Metabolite Analysis. A commercially available COSMO(+), chemically coated with a cationic polymer, capillary (50 μm i.d. × 110 cm) (Nacalai Tesque, Kyoto, Japan) was used as the separation capillary. A 50 mM ammonium acetate solution (pH 8.5) was the electrolyte for CE separation. Prior to the first use, a new capillary was flushed successively with the running electrolyte, 50 mM acetic acid (pH 3.4), and then the electrolyte again for 20 min each. Before each injection, the capillary was equilibrated for 2 min by flushing with 50 mM acetic acid (pH 3.4) and then for 5 min by flushing with the running electrolyte.[20]

A sample solution (30 nL) was injected at 50 mbar for 30 s, and −30 kV of voltage was applied. The capillary temperature was thermostated to 20 °C, and the sample tray was cooled to below 5 °C. The Agilent 1100 series pump equipped with a 1:100 splitter was used to deliver 10 μL/min of 5 mM ammonium acetate in 50% (v/v) methanol–water containing 0.1 μM Hexakis to the CE interface where it is used as a sheath liquid around the outside of the CE capillary to provide a stable electrical connection between the tip of the capillary and the grounded electrospray needle.

ESI-TOFMS was conducted in the negative ionization; the capillary voltage was set at 3500 V. For TOFMS, the fragmenter, skimmer, and Oct RFV voltage was set at 100, 50, and 200 V, respectively. A flow rate of drying nitrogen gas (heater temperature, 300 °C) was maintained at 7 L/min. Automatic recalibration

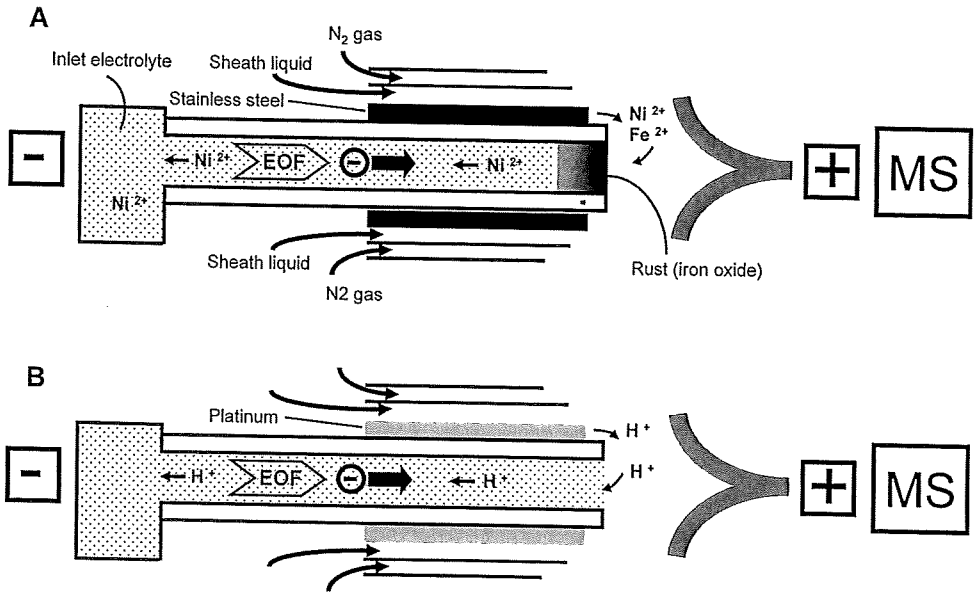

Figure 2. Schematic of anion analysis by the CE-MS in the negative mode using the CE-ESI-MS sprayer with (A) the stainless steel needle and (B) the platinum needle. (A) Metal ions like Fe^{2+} and Ni^{2+} were electrochemically generated from the stainless steel needle at the anode (pH 6.9) and moved into the separation capillary. Fe^{2+} was oxidized (forming rust) and plugged at the capillary outlet due to high electrolyte pH (8.5), while Ni^{2+} migrated toward the capillary inlet (cathode). Anions exhibiting high chelating properties with metal ions formed complexes when encountering Ni^{2+} or iron oxides. (B) In the platinum needle, water oxidation ($2H_2O \rightarrow 4H^+ + O_2\uparrow + 4e^-$) occurred at the anode and, thus, anionic metabolites did not encounter the metal ions.

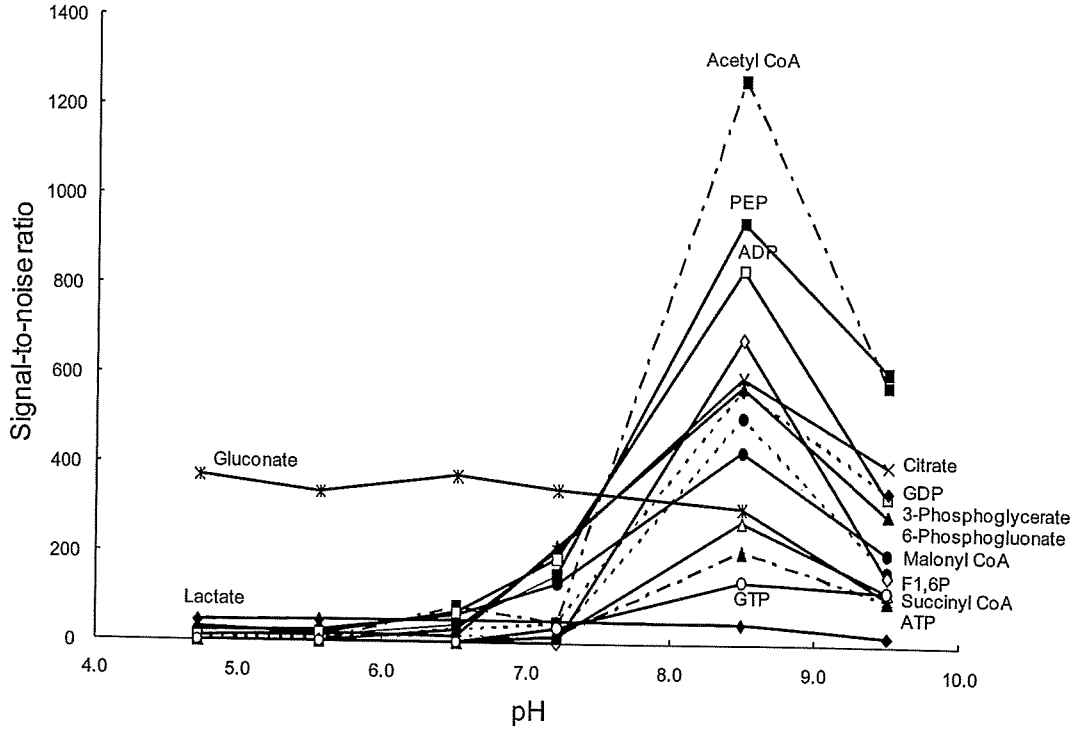

Figure 3. Effect of electrolyte pH on the sensitivity (signal-to-noise ratio) of anions. Experimental conditions: ESI spray needle, platinum; electrolyte, 50 mM ammonium acetate; other experimental conditions as in Figure 1.

of each acquired spectrum was performed using reference masses of reference standards ([^{13}C isotopic ion of deprotonated acetic acid dimer ($2CH_3COOH - H$)]$^-$, m/z 120.03841), and ([Hexakis + deprotonated acetic acid ($CH_3COOH - H$)]$^-$, m/z 680.03554). Exact mass data were acquired at a rate of 1.5 spectra/s over a 50−1000 m/z range.

Raw CE-TOFMS data were processed using software developed in-house for the quantification of metabolites.[13,25,26] All target metabolites were identified by matching their m/z values and migration times with those of standard compounds. For overall data analysis, three-dimensional representation of CE-TOFMS data was produced using MZmine2 software[27,28] (http://mzmine.sourceforge.net/).

(25) Baran, R.; Kochi, H.; Saito, N.; Suematsu, M.; Soga, T.; Nishioka, T.; Robert, M.; Tomita, M. *BMC Bioinf.* **2006**, *7*, 530.

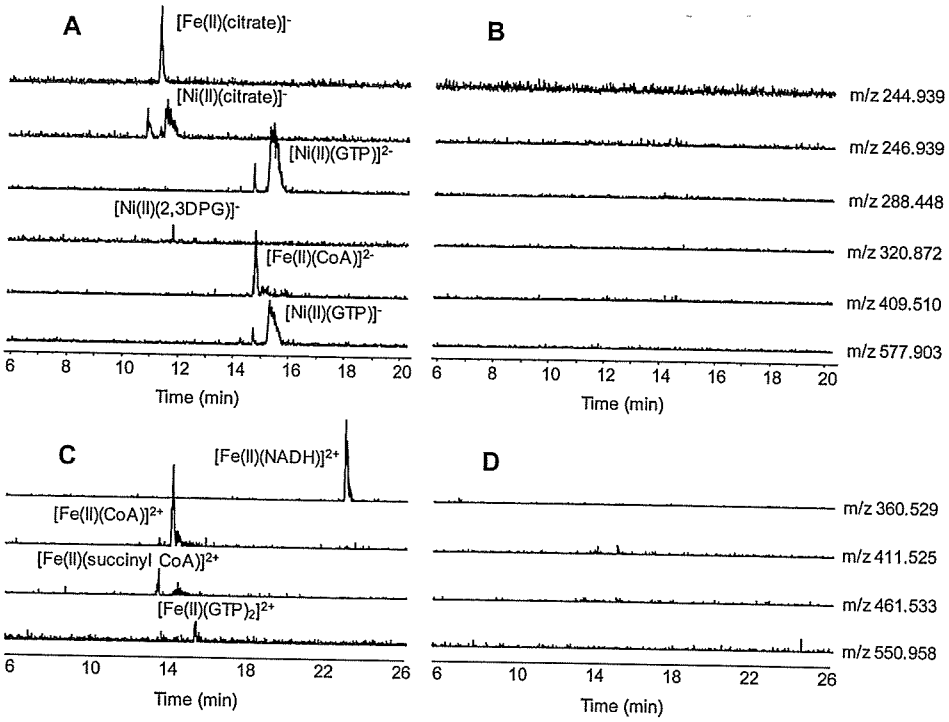

Figure 4. Abundance of metal–anion complexes in the analysis of 43 anionic metabolite standards using CE-TOFMS in the negative mode and negative ionization detection with (A) the stainless steel needle and (B) the platinum needle and positive ionization detection with (C) the stainless steel needle and (D) the platinum needle. Experimental conditions: the names of 43 anionic metabolite standards are listed in Table 1; the standard concentration was 50 μmol/L each; in the positive TOFMS detection, the ion polarity was switched to positive and the capillary voltage was set at 4000 V; other experimental conditions are the same as in Figure 1.

RESULTS AND DISCUSSION

Prevention of Capillary Plugging by Use of a Platinum ESI Needle. The sheath flow CE-MS method with negative mode using a cationic polymer-coated capillary demonstrated impressive performance for anion analysis.[13,20] However, the sensitivities of several anions were considerably poor. Moreover, migration times of every analyte immediately became longer, and the capillary frequently clogged. Removing the polyimide film, we examined a clogged capillary using a microscope and found that the capillary outlet became plugged with a rustlike precipitate. To identify it, we investigated its solubility using several organic solvents and acids including chloroform, isopropanol, acetone, acetonitrile, hydrochloric acid, hydronitric acid, and hydrosulfuric acid. Since it was only soluble in hydrochloric acid, it was identified as a transition metal having a high ionization tendency like iron and nickel.

Although the original Agilent CE-ESI-MS spray needle is made from SST316Ti stainless steel, it exhibited high ionization tendency and, thus, was oxidized to metal ions by electrolysis, resulting in a plug at the capillary outlet. To confirm this, we attached the following three types of spray needles to the Agilent ESI sprayer: normal- and passivated-SST316Ti stainless steel and platinum. Using these spray needles, we performed the CE-MS analyses with the negative mode and checked the capillary outlet with a microscope after 5, 10, and over 40 runs, respectively.

With the two needles made from the stainless steel, both the capillary outlets became plugged with precipitates (rust) after five runs and the rust grew thicker with the number of analysis performed, indicating that electrochemical oxidation of the stainless steel occurred. However, the use of the platinum needle resulted in no plugging for 100 runs. This is consistent with previous reports that platinum wire used as the CE-MS ESI electrode protects against electrode corrosion.[29–32] As Smith and Moini[31] reported, when a stainless steel wire was used as the anode, the oxidation of iron ($Fe \rightarrow Fe^{2+} + 2e^-$) (perhaps Ni, Cr, and Ti) replaced the oxidation of water ($2H_2O \rightarrow 4H^+ + O_2\uparrow + 4e^-$) by electrolysis, resulting in corrosion of the Fe and formation of Fe^{2+}. However, platinum wire only caused electrochemical oxidation of water, and bubble formation occurred at the anodic end.

The robustness of the CE-MS method with the negative mode using the SST316Ti stainless steel needle and platinum needle was further investigated. With the stainless steel needle, both capillary clogging with rust and significant corrosion at the tip of the needle occurred (Figure 1A) and the current fully dropped after 167 runs (Figure 1C). For the platinum needle, although a slight current drop and migration time fluctuation were observed (Figure 1C), it enabled over 545 successive analyses without capillary clogging and corrosion of the needle (Figure 1B). While Smith and Moini used iron wire, instead of platinum wire, as the anode to eliminate gas bubble formation in their sheathless CE-

(26) Hirayama, A.; Kami, K.; Sugimoto, M.; Sugawara, M.; Toki, N.; Onozuka, H.; Kinoshita, T.; Saito, N.; Ochiai, A.; Tomita, M.; Esumi, H.; Soga, T. *Cancer Res.* **2009**, *69*, 4918–4925.
(27) Katajamaa, M.; Oresic, M. *BMC Bioinf.* **2005**, *6*, 179.
(28) Katajamaa, M.; Miettinen, J.; Oresic, M. *Bioinformatics* **2006**, *22* (5), 634–636.
(29) Cao, P.; Moini, M. *J. Am. Soc. Mass Spectrom.* **1997**, *8*, 561–564.
(30) Herring, C. J.; Qin, J. *Rapid Commun. Mass Spectrom.* **1999**, *13*, 1–7.
(31) Smith, A. D.; Moini, M. *Anal. Chem.* **2001**, *73*, 240–246.
(32) Van Berkel, G. J.; Asano, K. G.; Schnier, P. D. *J. Am. Soc. Mass Spectrom.* **2001**, *12*, 853–862.

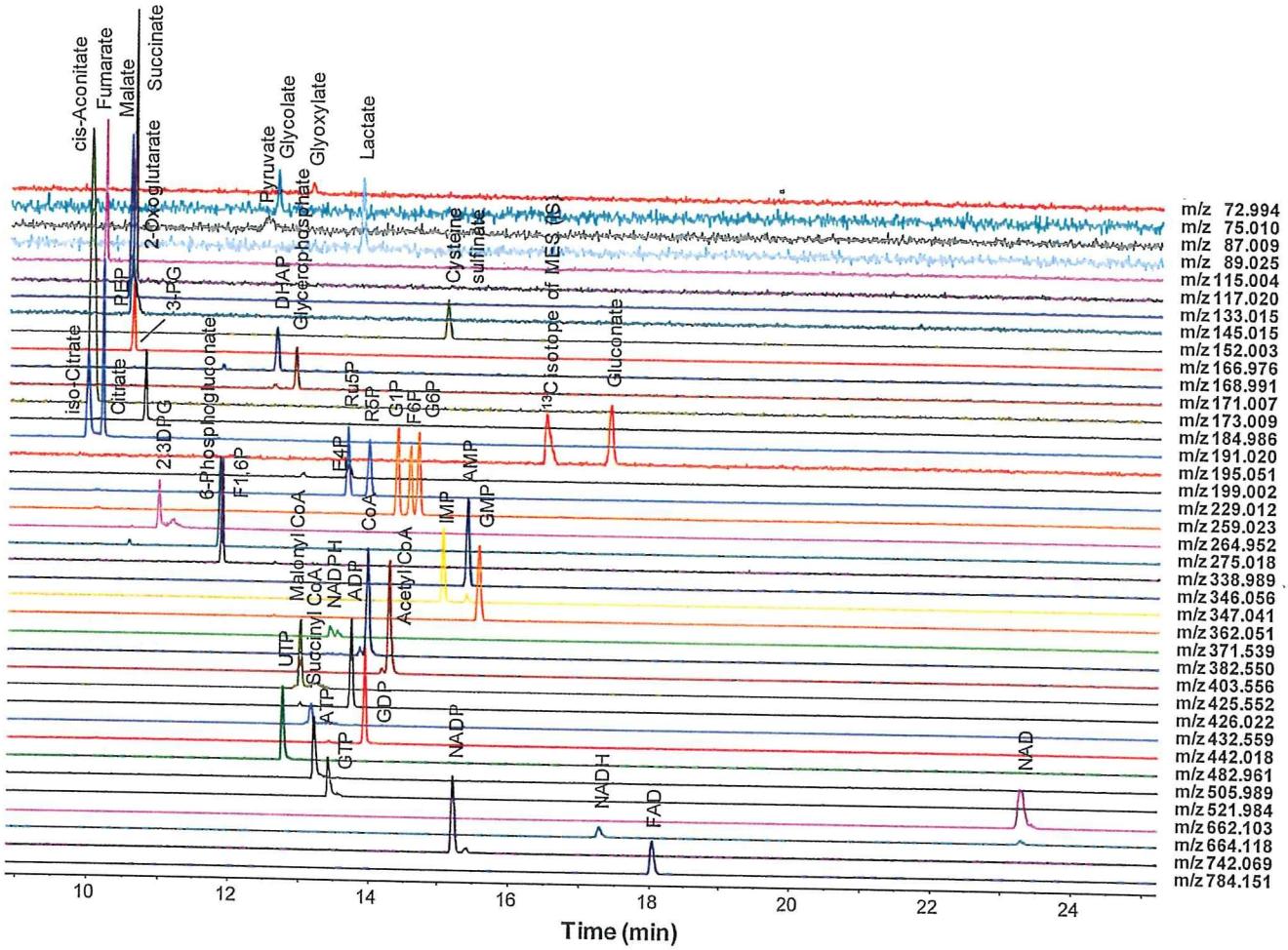

Figure 5. Selected CE-TOFMS ion electropherograms for a standard mixture of anionic metabolites in the components of glycolysis, pentose phosphate, and the TCA pathways obtained by the CE-ESI-MS sprayer attached with a platinum needle. Experimental conditions: standard concentration, 10 μmol/L each; other experimental conditions as in Figure 1. Abbreviations: PEP, phosphoenolpyruvate; DHAP, dihydroxyacetone phosphate; 3PG, 3-phosphoglycerate; E4P, erythrose 4-phosphate; Ru5P, ribulose 5-phosphate; R5P, ribose 5-phosphate; G1P, glucose 1-phosphate; F6P, fructose 6-phosphate; G6P, glucose 6-phosphate; 2,3DPG, 2,3-diphosphoglycerate; F1,6P, fructose 1,6-diphosphate; NADPH, reduced nicotinamide adenine dinucleotide phosphate; NADP, nicotinamide adenine dinucleotide phosphate; FAD, flavin adenine dinucleotide.

MS system,[31] our results indicate that bubble formation generated by the platinum needle had no effect on the analysis in the sheath flow CE-MS system.

Sensitivity Differences between the Stainless Steel Needle and the Platinum Spray Needle in Anion Analysis. There was another difficulty in analyzing anionic metabolites by the CE-MS method with the negative mode using the ESI sprayer equipped with the SST316Ti stainless steel needle. Several carboxylic acids and phosphorylated compounds such as malate, 2-oxoglutarate, 3-phosphoglycerate (3PG), citrate, isocitrate, gluconate, 2,3-diphosphoglycerate (2,3DPG), uridine 5′-triphosphate (UTP), adenosine 5′-triphosphate (ATP), guanosine 5′-triphosphate (GTP), reduced nicotinamide adenine dinucleotide (NADH), coenzyme A (CoA), and acetyl- and malonyl-CoA with a concentration below a few micromolar were not detected. However, all the anions were detected as well-defined peaks with the platinum needle.

Many carboxylic acids and nucleotides such as citrate, malate, ATP, GTP, and NADH are complexing agents,[33–38] which display high stability constants for transition metals. For phosphorylated saccharides and CoAs, stability constants for transition metals have not been frequently reported. However, as metal–phosphate affinity is well-known[33,35,39,40] and these characteristics are frequently utilized in phoshoproteomics studies,[41,42] most phosphorylated compounds will likely interact with transition metals.

Experiments show sensitivity differences between the two needles for metal-chelating carboxylic acids, and phosphorylated anions are observed (Table 1). Conversely, pyruvate, lactate, and fumarate exhibit little or no stability constants for transition metals,[34] and their sensitivities were independent of the needle type. Unlike NADH, nicotinamide adenine dinucleotide (NAD^+)

(33) Toyokuni, S. *Free Radicical Biol. Med.* **1996**, *20*, 553–566.
(34) Soga, T.; Gordon, R. A. *J. Chromatigr., A* **1997**, *767*, 223–230.
(35) Kowaltowski, A. J.; Vercesi, A. E. *Free Radical Biol. Med.* **1999**, *26*, 463–471.
(36) Canaviri, E. C.; Feliz, M. R.; Capparelli, A. L. *Transition Met. Chem.* **1992**, *17*, 446–448.
(37) Champeil, P.; Rigaud, J. L.; Gary-Bobo, C. M. *Proc. Natl. Acad. Sci. U.S.A.* **1980**, *77*, 2405–2409.
(38) Lvovich, V.; Scheeline, A. *Arch. Biochem. Biophys.* **1995**, *320*, 1–13.
(39) Takebayashi, Y.; Mitsuma, R.; Imanari, T. *Anal. Sci.* **1987**, *3*, 569–572.
(40) Ziemniak, S. E.; Jones, M. E.; Combs, K. E. S. *J. Solution Chem.* **1989**, *18*, 1133–1152.
(41) Stensballe, A.; Andersen, S.; Jensen, O. N. *Proteomics* **2001**, *1*, 207–222.
(42) Kokubu, M.; Ishihama, Y.; Sato, T.; Nagasu, T.; Oda, Y. *Anal. Chem.* **2005**, *77*, 5144–5154.

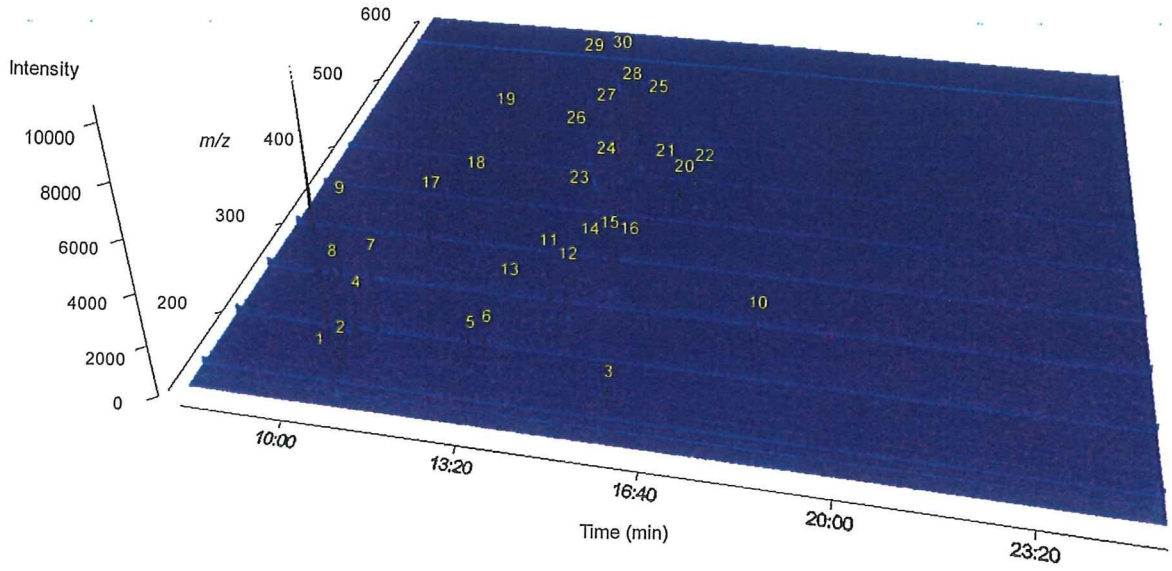

Figure 6. Three-dimensional representation (total ion electropherogram) for the analysis of a standard mixture of anionic metabolites found in glycolysis, pentose phosphate, and the TCA pathways. Results were obtained by the CE-TOFMS in the negative mode using the CE-ESI sprayer with a platinum needle. Experimental conditions: standard concentration, 50 μmol/L each; other experimental conditions are the same as in Figure 1. Peaks: 1, malate; 2, 2-oxoglutarate; 3, cysteine sulfinate; 4, PEP; 5, DHAP; 6, glycerophosphate; 7, 3PG; 8, isocitrate; 9, citrate; 10, gluconate; 11, E4P; 12, Ru5P; 13, R5P; 14, G1P; 15, F6P; 16, G6P; 17, 2,3DPG; 18, 6-phosphogluconate; 19, F1,6P; 20, AMP; 21, IMP; 22, GMP; 23, NADPH; 24, CoA; 25, acetyl CoA; 26, malonyl CoA; 27, ADP; 28, GDP; 29, UTP; 30, ATP.

does not form a complex with the Fe^{2+} ion;[38] thereby, NAD^+'s sensitivity is most similar between the two needles. These facts indicate that the anions' metal-chelating properties likely affect their detection sensitivities.

Effect of Generated Metal Ions on Sensitivity in Measurement of Anionic Metabolites. To investigate the hypothesis that anionic metabolites exhibiting high stability constants for metal ions might form complexes with the iron oxides generated by the stainless steel needle, the separation capillary was cut into five pieces (each 20 cm) and analyzed by ICP-MS. The ICP-MS analysis detected a 10.4 ppb level of Fe in the tip of the capillary outlet (the anode side), which identified the rust as iron oxide, but no metals in other regions of the capillary. Surprisingly, nickel was detected in the capillary inlet electrolyte, and its concentration dramatically increased (0.96 μg/L at 1 h and reached 3.08 μg/L at 2 h) even when no sample was injected. This indicates that nickel ion migrated from the anode to the inlet electrolyte vial. However, no such phenomena were observed when using the platinum needle.

It is, therefore, assumed that, with the stainless steel needle (Figure 2A), iron and nickel ions generated at the anode due to electrolysis moved to the capillary outlet in the sheath liquid (pH 6.9) and iron oxides formed because of the high pH (pH 8.5)[20] (Figure 3). Simultaneously, Ni^{2+} ions migrated toward the cathode without precipitation and then collected in the capillary inlet electrolyte vial. In this manner, injected anionic metabolites encountered Ni^{2+} in the separation capillary or the iron oxides at the capillary end and formed metal–anion complexes (Figure 2A). In the case of the platinum needle, water oxidation ($2H_2O \rightarrow 4H^+ + O_2\uparrow + 4e^-$) occurred at the anode due to its low ionization tendency and anionic metabolites did not encounter the metal ions and were fully detected by the mass spectrometer (Figure 2B).

The formation of metal–anion complexes during the CE-MS analysis was also confirmed. As listed in Table 1, when the stainless steel needle was used, a significant drop in sensitivity was observed for many anions including citrate, 2,3DPG, GTP, CoA, succinyl CoA, and NADH. For these anions, the formation of all nickel(II)– and iron(II)–anion complexes was analyzed by the CE-TOFMS method. In the negative ionization TOFMS method, nickel(II)– and iron(II)–anion complexes such as $[Fe(II)-(citrate)]^-$, $[Ni(II)-(citrate)]^-$, $[Ni(II)-(GTP)]^{2-}$, $[Ni(II)-(2,3DPG)]^-$, $[Fe(II)-(CoA)]^{2-}$, and $[Ni(II)-(GTP)]^-$ were detected with the stainless steel needle (Figure 4A). Moreover, positively charged nickel(II)– and iron(II)–anion complexes such as $[Fe(II)-(NADH)]^{2+}$, $[Fe(II)-(CoA)]^{2+}$, $[Fe(II)-(succinyl\ CoA)]^{2+}$, and $[Fe(II)-(GTP)_2]^{2+}$ were present in the positive ionization TOFMS detection (Figure 4C). These results indicate that all the anions formed complexes with nickel(II) and iron(II) ions with the stainless steel needle. No metal complexes were observed with the platinum needle (Figure 4B,D).

It was found, however, that the sensitivities for pyruvate, lactate, and fumarate were equivalent using either the stainless steel or platinum needle (Table 1). Although a trace of $[Fe(II)-(pyruvate)_3]^-$ was detected with the stainless steel needle, neither these nickel(II)– nor iron(II)–anion complexes were detected with either needle. These results indicate that with the stainless steel needle, anions exhibiting high stability constants with metals formed complexes with nickel and iron ions generated by electrolysis, resulting in a significant decrease in detection sensitivity.

Effect of Electrolyte pH on Rust Formation and Sensitivity in the CE-MS System. Given that iron ions generated from the stainless steel needle precipitated when encountering the alkaline electrolyte (pH 8.5), they are expected to be dissolved under acidic conditions. To confirm this, iron oxide formation was studied over

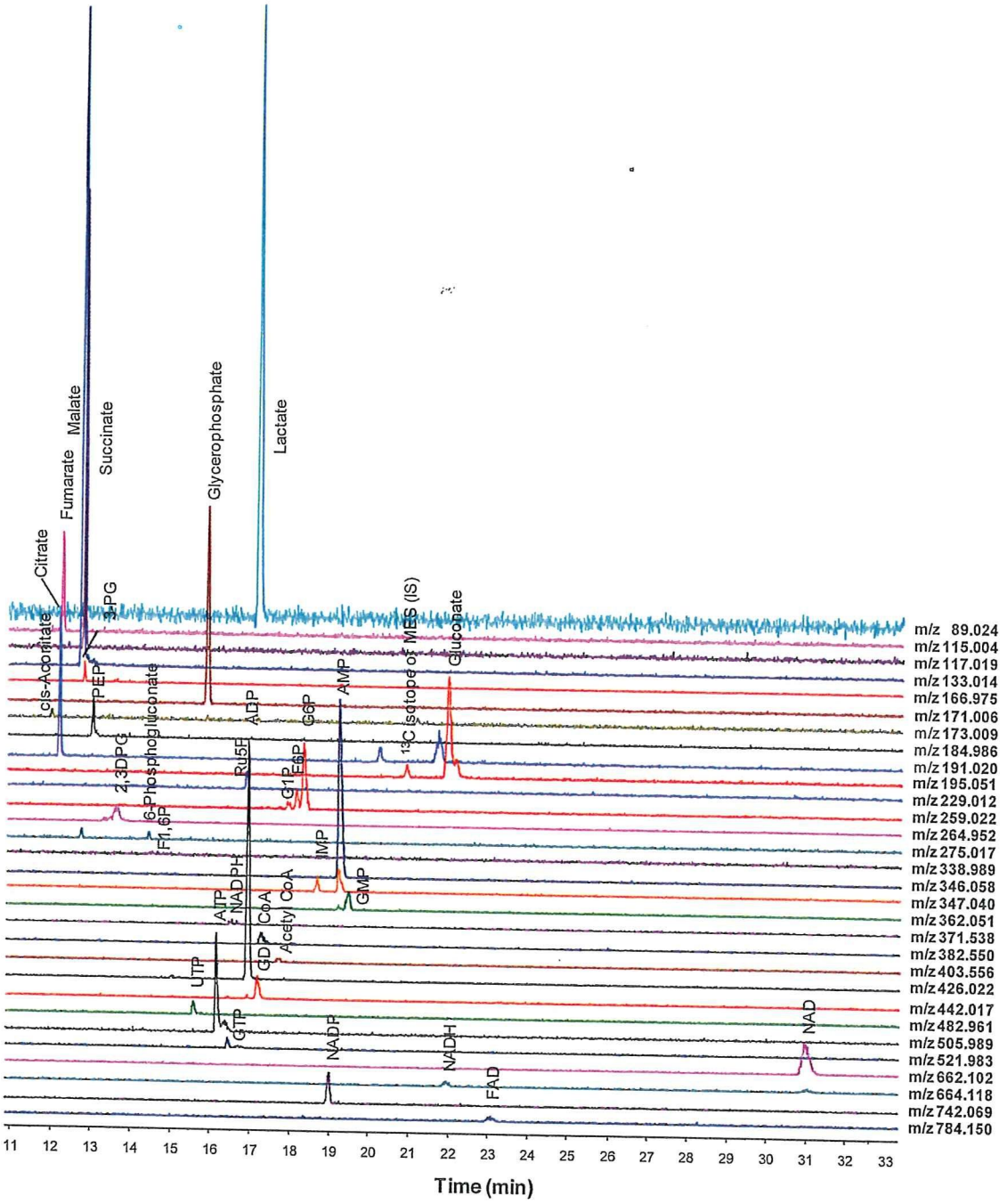

Figure 7. Selected CE-TOFMS ion electropherograms for components of glycolysis, pentose phosphate, and the TCA pathways in mouse liver. Experimental conditions are the same as in Figure 1.

pH range 4.7–9.5 using 50 mM ammonium acetate as the electrolyte and the stainless steel needle. At a pH value of 7.5, both rust development at the capillary end and corrosion of the stainless steel needle were observed. At pH 5.0, although corrosion of the needle was still observed, no iron oxide was formed. After the voltage was applied (no sample injection) for 2 h at the pH 5.0, metals at the capillary inlet electrolyte were analyzed by ICP-MS. Fe, Ni, and Ti, some components of the SST316Ti stainless steel, were detected at amounts of 1.23, 0.88, and 0.24 μg/L, respectively, which strongly implies that these metal ions were generated by electrolysis and migrated toward the cathodes.

Nevertheless, decreasing electrolyte pH had a significant effect on the detection sensitivity of anionic species (Figure 3). Below pH 7.5, although the reason was unclear, a considerable deterioration in the peak shape and extended migration time of many anions including phosphorylated substrates, nucleotide di- and triphosphates, and CoAs were observed, which resulted in substantial reduction in their detection sensitivity. Particularly, neither nucleotide triphosphates nor CoAs were detected below pH 6.5. Sensitivities of anions also decreased when the pH was increased to pH 9.5. Maximal sensitivities for most anions were obtained at pH 8.5 (Figure 3). This result was independent of the ESI needle type used. Reduction of sensitivity depending on the pH may be caused by the interaction between these compounds and the cationic coated polymer on the capillary wall, though further investigation is necessary.

In conclusion, there is no pH that can be used with the stainless steel needle to both prevent iron oxide formation and maintain

Table 2. Metabolite Amount, Reproducibility, and Recovery in Mouse Liver Analysis

compound	amount (nmol/g)	RSD (n = 12) (%)	recovery rate (average, n = 5) (%)
glyoxylate	nd[a]		106
glycolate	nd		117
pyruvate	nd		138
lactate	2440	5.7	67
fumarate	247	8.4	99
succinate	526	4.9	65
malate	1250	2.6	53
2-oxoglutarate	nd		94
cysteine sulfinate	nd		101
PEP	44	7.8	96
DHAP	nd		100
glycerophosphate	1310	3.9	97
cis-aconitate	6.0	15.6	141
3-phosphoglycerate	159	5.0	103
isocitrate	nd		103
citrate	264	6.1	89
gluconate	675	4.5	109
E4P	nd		114
Ru5P	68	11.1	101
R5P	nd		98
G1P	34	12.7	97
F6P	98	7.0	92
G6P	392	4.7	95
2,3DPG	215	5.1	93
6-phosphogluconate	23	21.9	97
F1,6P	22	15.8	92
AMP	1240	2.1	96
IMP	81	7.9	98
GMP	143	4.8	93
NADPH (divalent)	66	16.5	146
CoA (divalent)	68	10.0	132
acetyl CoA (divalent)	14	15.4	96
malonyl CoA (divalent)	nd		110
ADP	1500	4.7	88
succinyl CoA (divalent)	nd[a]		58
GDP	181	3.0	94
UTP	89	15.3	94
ATP	889	3.8	120
GTP	149	6.2	183
NAD	494	3.7	93
NADH	166	7.2	114
NADP	184	4.9	90
FAD	47	7.5	92

[a] nd, not detected.

peak shape for necessary detection sensitivity. For the platinum needle, pH 8.5 was found optimal.

Method Validation. Figure 5 illustrates selected ion electropherograms of the 43 anionic metabolite standards in the components of glycolysis, pentose phosphate, and the tricarboxylic acid (TCA) pathways obtained by the sheath flow CE-TOFMS with the negative mode using the platinum spray needle. A three-dimensional presentation (total ion electropherogram) is shown in Figure 6. This analysis will be particularly important to analyze unknown metabolites. This approach provided much better sensitivity and, thereby, contributed to excellent performance, compared to the previous method. Most of compounds were detected at their monovalent deprotonated molecular $[M - H]^-$ ions, while intensity in the divalent $[M - 2H]^{2-}$ ion of NADPH and CoA compounds was higher than that in monovalent ion.

The reproducibility, linearity, and sensitivity of this method are listed in Table 1. Practical reproducibility was obtained for all anionic species with relative standard deviation (RSD) values (n = 8) for migration times between 0.5 and 1.1% and for peak areas better than 10% except for glyoxylate, glycolate, succinyl CoA, GTP, and FAD, as indicated in the table. The calibration curves for all species were linear at 1, 2, 5, 10, 20, 50, 100, and 200 μmol/L with correlation coefficients between 0.980 and 0.999.

This method significantly improved the sensitivity of many anions. Although the previous method using the stainless steel needle was unable to detect 20 μmol/L of CoA, the use of the platinum needle dramatically improved sensitivity and enabled the detection of 1 μmol/L of CoA. Moreover, the sensitivities for the anions exhibiting high stability constants for metal ions such as citrate, 2,3DPG, GTP, and NADH were 63-, 35-, 15-, and 11-fold superior to those obtained by the stainless steel needle, respectively. Also several-fold better sensitivities for many anions including malate, 2-oxoglutarate, *cis*-aconitate, isocitrate, ADP, ATP, GDP, UTP, and succinyl-, acetyl-, and malonyl CoA were obtained.

Anions exhibiting low stability constants with metals such as pyruvate and lactate showed similar sensitivities between the two needles. Overall, the concentration detection limits for most of the anions, except for glyoxylate, glycolate, pyruvate, and lactate, were between 0.03 and 1.1 μmol/L with a pressure injection of 50 mbar for 30 s (30 nL); i.e., mass detection limits ranged from 0.8 to 33 fmol, at a signal-to-noise ratio of 3.

Analysis of Mouse Liver Metabolites in the Central Carbon and Energy Metabolism. The utility of the CE-TOFMS method was demonstrated by the simultaneous analysis of the central carbon and energy metabolism components extracted from mouse liver. There are more than 40 anionic intermediates that belong to several categories of chemical compounds: phosphorylated saccharides, phosphorylated carboxylic acids, carboxylic acids, nucleotides, and cofactors. Simultaneous, quantitative, and direct analysis of these compounds is a challenging analytical problem. Figure 7 shows the results for the analysis of the central carbon and energy metabolic components extracted from mouse livers obtained by the CE-TOFMS method. The 32 components were identified by comparing their molecular weights and migration times with those of metabolite standards, and their amounts were quantified by their standard calibration curves (Table 1). The relative standard deviations (n = 12) for the amounts of identified compounds in the mouse liver sample were better than 6% except for small compounds. To investigate quantification accuracy and ion suppression effect in this system, we analyzed mouse liver samples spiked with 20 μM of each standard and calculated the recovery (Table 2). Except for a few metabolites, the recovery rates of most metabolites in the CE-TOFMS approach were between 80 and 130%. Although the reason was not clear, the recovery rate of GTP was unusually high (183%). Considering the good reproducibility and recovery rates, the CE-TOFMS method in the negative mode using the platinum spray needle seems to be scarcely affected by the ion suppression effect and it enables sufficient quantitative analysis of most anionic intermediates in the central carbon and energy metabolic pathways extracted from mouse liver samples.

CONCLUSIONS

A negatively charged metabolites profiling approach based on sheath flow CE-TOFMS with a negative mode is described. The material of the ESI spray needle had a significant effect

on the measurement of anions. Due to electrolysis, the stainless steel sprayer needle was easily oxidized and generated metal ions, which caused corrosion of the needle and capillary clogging. Moreover, metal ions formed complexes with many anions, significantly decreasing detection sensitivity. The key to success was using a platinum spray needle, a low ionization tendency metal, which prevented both generation of metal ions and corrosion of the needle caused by electrolysis. Compared with the previously reported techniques, this method has several advantages: (1) it is able to integrate two CE-MS methods into one method, and thereby, all types of anionic components such as phosphorylated saccharides, phosphorylated carboxylic acids, carboxylic acids, CoA compounds, nucleotides, and nicotinamide adenine dinucleotides are simultaneously analyzed; (2) more than several-fold increased sensitivities of anions which exhibit high metal chelating properties are obtained; and (3) the present method provides improved reproducibility, quantification accuracy, and method robustness (i.e., capillary lifetime). Its utility was demonstrated by the simultaneous and quantitative analysis of the central carbon and the energy the metabolic intermediates extracted from mouse livers. These results indicate that the proposed CE-TOFMS method can be useful for the comprehensive analysis of anionic species in a wide range of application areas.

ACKNOWLEDGMENT

We thank Akiyoshi Hirayama and Dr. Masahiro Sugimoto, Institute for Advanced Biosciences, Keio University, and Takamasa Ishikawa, Human Metabolome Technologies Inc., for technical support, and Dr. David N. Heiger, Agilent Technologies, for critical reading of the manuscript. This work was supported in part by grants for the Health and Labour Sciences Research Grants entitled "Research on Risk of Chemical Substances" and "Research on Biological Markers for Drug development", by a Grant-in-Aid for Creative Scientific Research 17GS0419 from the Japan Society for the Promotion of Science, by a grant from the Global COE Program entitled "Human Metabolic System Biology", and by a Grant-in-Aid for Scientific Research on Priority Areas "Life surveyor" and "Systems Genomes" from the Ministry of Education, Culture, Sport, Science, and Technology (MEXT) in Japan as well as by research funds from Yamagata prefectural government and Tsuruoka city.

Received for review March 31, 2009. Accepted May 31, 2009.

AC900675K

はじめに
Introduction

曽我朋義
Tomoyoshi SOGA
慶應義塾大学先端生命科学研究所

トランスクリプトミクス，プロテオミクス，メタボロミクス等のオミクス研究は細胞や生体内の多数の構成成分の変化をバイアスをかけない手法により網羅的に探索し，生命現象を包括的に理解しようとするものである．従来の仮説検証型の科学に対して，オミクスは網羅的なデータ解析によって背後に隠れている因子をみつけ出そうとする仮説発見型研究であり，だれも予想もしていなかった大発見をもたらす可能性を秘める．

今回はポストゲノム医学の新しい研究手法として最近注目を集めているメタボロミクスについて特集した．生物の活動は代謝とよばれるさまざまな酵素による化学反応の連鎖によって支えられている．代謝のおもな役割は外界から取り入れた物質をエネルギー(ATP)や，DNA，蛋白質などの生体高分子の前駆体(ヌクレオチド，アミノ酸など)あるいは脂質などに変換することである．代謝によって生産された代謝中間体や代謝産物の総称をメタボロームとよび，微生物で数百，哺乳動物で数千，植物で数万種類の代謝産物が存在するといわれている．

代謝物質は，物理的化学的性質が非常に似かよったものから，まったく異なるものまで数百種から数万種類存在するため，ひとつの分析法ですべてのメタボロームを測定することはいまだ困難である．しかし，ガスクロマトグラフィ-質量分析計(GC/MS)，高速液体クロマトグラフィ-質量分析計(LC-MS)，キャピラリー電気泳動-質量分析計(CE-MS)など定量的なメタボローム測定法が確立され，近年急速にメタボロミクスが医薬分野の基礎から応用研究に用いられるようになった．通常，代謝は高度に調節され，安定化されているが，代謝の異常で多くの疾患が引き起こされることや，癌細胞が異常な代謝を示すことなどは広く知られており，癌や疾病の機序解明や創薬開発には包括的に代謝を理解することが必要である．

本特集では，医薬分野で興味深いメタボローム解析を展開されている研究者に最新の成果を簡単に紹介していただいた．メタボロミクスはまだ生まれたばかりの方法論である．意欲的な人材がこの研究分野に参画し，新天地を切り開いてくれることを期待したい．

ヒト癌組織のメタボローム解析

Metabolome analysis of human tumor tissues

平山明由(写真)　曽我朋義
Akiyoshi HIRAYAMA and Tomoyoshi SOGA
慶應義塾大学先端生命科学研究所メタボローム解析グループ

◎キャピラリー電気泳動-質量分析装置(CE-MS)を用いたメタボローム測定法は，各種サンプル中に含まれるイオン性低分子代謝物の網羅的測定に適している．とくに解糖系，ペントースリン酸回路，TCA回路をはじめとして，アミノ酸代謝やプリン，ピリミジン代謝など，エネルギー代謝に関与する代謝物のほとんどはイオン性であることから，本法はエネルギー代謝を解明するうえで有用なツールになると考えられる．本稿ではCE-MSによるメタボローム解析を用いて，癌の微小環境における特殊なエネルギー代謝を明らかにした研究成果を紹介したい．

Key word：キャピラリー電気泳動-質量分析装置(CE-MS)，ワーバーグ効果，フマル酸呼吸

癌は周知のとおり，増殖，浸潤，転移を繰り返し，結果的にヒトを死に至らしめる疾患であるが，これまでに癌組織のエネルギー代謝を包括的に調べた研究例はほとんどない．通常，癌が増殖するためには膨大なエネルギー(ATP)が必要になるはずであるが，これら必要なエネルギーがどのように産生され，供給されているのかについては未知の部分も多い．メタボロームは生体内の代謝産物の総体を示す用語であるが，著者らはこれまでに，おもにキャピラリー電気泳動-質量分析装置(capillary electrophoresis-mass spectrometer：CE-MS)を用いたメタボローム解析を，微生物[1,2]，植物[3]，動物[4]などのサンプルに適用してきた．CE-MSは解糖系，ペントースリン酸回路，TCA回路をはじめとして，アミノ酸代謝，プリン代謝やピリミジン代謝などのエネルギー代謝に必須な代謝物群の一斉定量に有用な測定法である(「サイドメモ」参照)．

本稿では，CE-MSを用いたメタボローム解析を癌の微小環境における代謝の解明に応用し，得られた成果[5]を紹介する．

低酸素と癌のエネルギー代謝

癌細胞が好気的条件下においてもミトコンドリアでの呼吸を使わずに，おもに解糖系によってエネルギー産生を行う現象はワーバーグ効果[6]とよばれ，これまでにさまざまな癌種において確認されている．癌には，肝癌や胃癌のように比較的酸素分圧の高い癌と，膵癌や大腸癌のように癌細胞のまわりに血管がほとんどない(酸素分圧の低い)タイプの癌が存在し，一般的には後者のほうが増殖能力は高いといわれている．癌が増殖するには

サイドメモ　CE-MS

キャピラリー電気泳動(capillary electrophoresis：CE)と質量分析装置(mass spectrometer：MS)を並列につないだ分析装置の略称．内径数十μmのキャピラリー(毛細管)の中に泳動液を満たし，両端に数十kVの高電圧を印加することによって，キャピラリー内の物質をその電荷と水和イオン半径に基づいて分離した後，質量分析装置に導入することによって，高分離・高感度に検出する分析手法である．

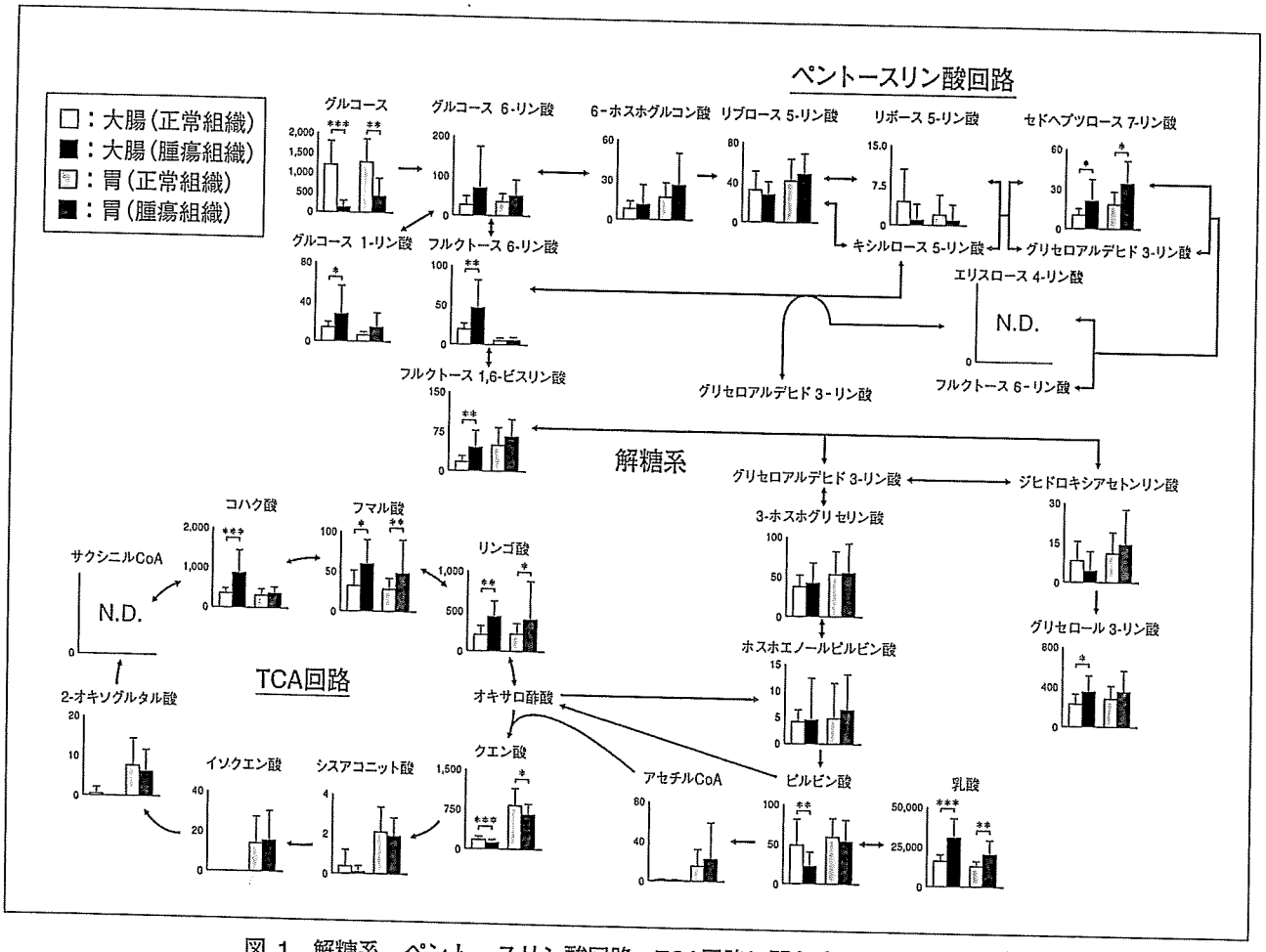

図 1　解糖系，ペントースリン酸回路，TCA回路に関与する代謝物の変動[5]
各代謝物量は 1 g 臓器当りの平均値±標準偏差で示してある．また，統計学的有意差の算出には Wilcoxon 検定を用いた．
*：$p<0.05$，**：$p<0.01$，***：$p<0.001$．

エネルギーとしての ATP が必要不可欠であるが，大部分の ATP は解糖系か酸化的リン酸化によって生産される．しかし，血管がないところで増殖する癌細胞は，解糖系に必要なグルコース量も酸化的リン酸化で必要な酸素も不足している．血流不足によって解糖系も酸化的リン酸化も制限された環境下においても増殖を続けられる癌細胞は，いったいそのエネルギーをどのように産生しているのであろうか．

そこで著者らは，キャピラリー電気泳動-飛行時間型質量分析装置(CE-TOFMS)を用いたメタボローム測定により，大腸癌および胃癌患者から採取した腫瘍組織および正常組織の代謝物質を一斉分析し，癌組織におけるエネルギー代謝のメカニズムの解明を試みた．

中心炭素代謝

今回，著者らは CE-TOFMS を用いたメタボローム測定によって，16 名の大腸癌患者，および 12 名の胃癌患者の腫瘍組織中から，約 800～1,100 種類の代謝物質由来と思われるピークを得た．そのうち，エネルギー代謝にとくに重要である解糖系，ペントースリン酸回路，TCA 回路の代謝中間体を代謝経路上にマッピングした結果を図 1 に示す．これらの代謝物に関しては標準物質を用いて各臓器 1 g 中の定量値を算出し，全サンプルの平均値をグラフに記載した．なお，グルコースに関しては液体クロマトグラフ-質量分析装置(LC-MS)を用いて定量値を算出した．

まず，腫瘍組織中のグルコース量はその正常組織中の量と比較して，大腸癌で約 1/10，胃癌では約 1/3 程度であった．さらに，これらは血中グルコース濃度と比較するとわずか 1/45(大腸癌)～1/13(胃癌)にしかならなかった(組織密度を 1 g/ml，血中グルコース濃度を 1 mg/ml と仮定した場合)．このことは生体内の癌が，最初に予想したと

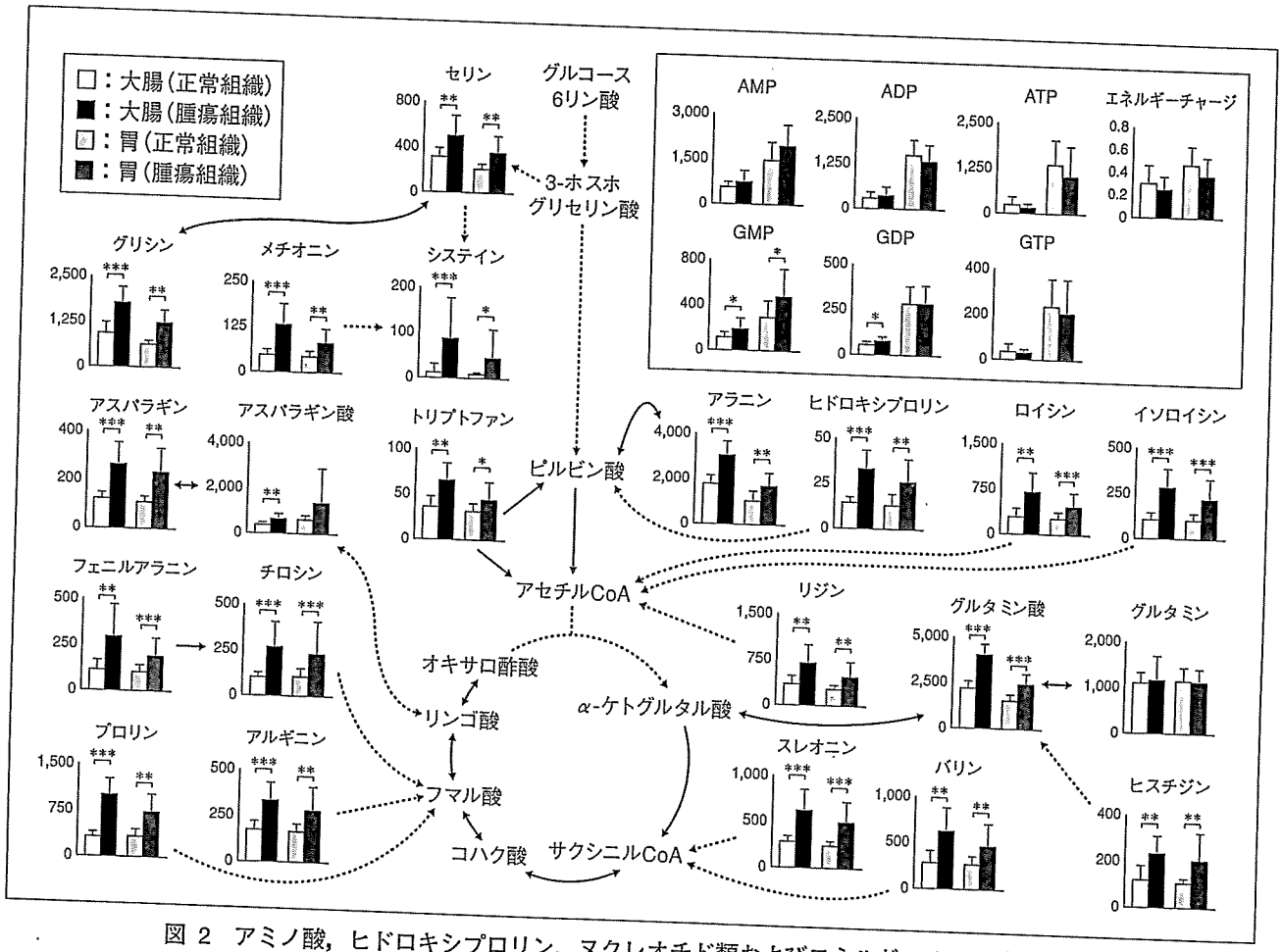

図 2　アミノ酸，ヒドロキシプロリン，ヌクレオチド類およびエネルギーチャージの変動[5]
各グラフの表示は図 1 と同じ．

おり血流の乏しい劣悪な環境下に存在していることを示唆している．一方で，解糖系の中間体物質量は非腫瘍組織と比べて同等かそれ以上であり，さらに解糖系の最終産物である乳酸量は両腫瘍組織において有意に高かった．このことから，Warburg が報告したように実際のヒトの腫瘍組織でも解糖系が亢進していることが明らかになった．

つぎに TCA 回路の代謝物に目を向けると，胃では正常，腫瘍組織とも TCA 回路の代謝中間体は一定量存在していたが，大腸では正常・腫瘍組織とも TCA 回路前半の代謝物(クエン酸からサクシニル CoA まで)がほとんど検出されておらず，ATP 量もきわめて低かった．大腸の酸素分圧は，胃のそれに比べて 1/5 程度という報告もあることから，おそらく大腸では正常組織も腫瘍組織も酸化的リン酸化反応はほとんど行われていないのではないかと推測される．

一方，TCA 回路後半の代謝物については癌特異的な傾向がみられた．とくに大腸の腫瘍組織において，TCA 回路の後半部分の代謝物(コハク酸，フマル酸，リンゴ酸)が有意に増加していた．この原因は謎であったが，寄生虫の呼吸にこの謎を解くヒントがあった．古くから嫌気性微生物や回虫などの寄生虫や二枚貝の一部では，嫌気的条件下でフマル酸呼吸とよばれる代謝によって ATP 産生が行われることが知られていた[7,8]．フマル酸呼吸は，電子伝達系における電子受容体として酸素の代りにフマル酸を用いて嫌気的に ATP を生成する反応であるが，その際に副生成物としてコハク酸を生じる．今回得られた大腸癌組織の結果においてもコハク酸が多く蓄積しており，嫌気的条件下での回虫の代謝パターンと類似していた．

一方，ある種の虫下し薬はフマル酸呼吸を阻害することが報告されており，著者らは虫下し薬を膵癌の培養細胞に添加すると癌細胞が死滅することをすでに実験で確かめている．これらを勘案した結果，現在のところ著者らは癌細胞もフマル酸呼吸かそれに類似した代謝によって ATP を産生

しているのではないかと考えている．

アミノ酸とヌクレオチド

図1に示したように，癌細胞では血流不足に伴い供給されるグルコース量も不足している．腫瘍組織はATP産生の一部をフマル酸呼吸に頼るとしても，それに必要なフマル酸はどこから供給されるのであろうか．図2に大腸および胃癌患者の正常，腫瘍組織のアミノ酸およびヌクレオチド量を示した．どちらの癌種においてもグルタミン以外のすべてのアミノ酸が有意に増加していた．血管新生が不十分な癌組織ではグルコース同様，血液からのアミノ酸の供給も不足していると考えられるため，これらのアミノ酸の増加は不思議である．

著者らは，必須アミノ酸も増加していること，ならびにコラーゲンの分解によって特異的に生成されることが知られているヒドロキシプロリン[9]量が増加していることから，腫瘍組織ではオートファージ[10,11]を活性化させることによりコラーゲンなどの周囲の蛋白質を積極的に分解し，ATPを生産するための前駆体としてアミノ酸を取り入れているのではないかと考えている．正常組織と腫瘍組織で唯一差のみられなかったグルタミンについては，グルタミノリシスという特殊な代謝がさまざまな癌種において活性化されている[12,13]ことがすでに知られている．つまり，癌細胞においてはグルタミンを特異的に消費する代謝経路が亢進しているために両組織間の差がなくなったものと考えられる．

最後に，大腸癌および胃癌の各組織におけるエネルギーチャージ[14]を比較した．興味深いことに，部分的にはまったく異なったエネルギー産生を行っているように思えたが，全体としてのエネルギーバランスは一定に保たれていることが証明された．

おわりに

本稿ではCE-MSを用いたメタボローム解析について，癌組織のエネルギー代謝の解明に応用した例をあげて紹介した．イオン性代謝物の一斉分析を可能にするCE-MSを用いて，著者らはすでに代謝調節メカニズムの解明，新規代謝経路の探索や各種バイオマーカーの探索など，基礎から応用に至るまでのさまざまなプロジェクトを推進し，成果を得つつある．本稿がCE-MSをはじめとしたメタボローム解析を理解していただく助けになれば幸いである．

謝辞：サンプル提供ならびにデータ解析に関してサポートをいただいた，国立がんセンター東病院の江角浩安病院長，小野塚博子博士，木下　平博士，斎藤典男博士，落合淳志博士，ならびに慶應義塾大学先端生命科学研究所の紙　健次郎氏，杉本昌弘博士，菅原真生氏，土岐尚子氏にこの場を借りて深謝致します．本研究は，厚生労働省癌研究助成金，文部科学省グローバルCOEプログラム“*In vivo* ヒト代謝システム生物学”，山形県および鶴岡市の支援によるものである．

文献

1) Ishii, N. et al.：Multiple high-throughput analyses monitor the response of E. coli to perturbations. *Science*, **316**：593-597, 2007.
2) Soga, T. et al.：Quantitative metabolome analysis using capillary electrophoresis mass spectrometry. *J. Proteome Res.*, **2**：488-494, 2003.
3) Sato, S. et al.：Simultaneous determination of the main metabolites in rice leaves using capillary electrophoresis mass spectrometry and capillary electrophoresis diode array detection. *Plant. J.*, **40**：151-163, 2004.
4) Soga, T. et al.：Differential metabolomics reveals ophthalmic acid as an oxidative stress biomarker indicating hepatic glutathione consumption. *J. Biol. Chem.*, **281**：16768-16776, 2006.
5) Hirayama, A. et al.：Quantitative metabolome profiling of colon and stomach cancer microenvironment by capillary electrophoresis time-of-flight mass spectrometry. *Cancer Res.*, **69**：4918-4925, 2009.
6) Warburg, O.：On the origin of cancer cells. *Science*, **123**：309-314, 1956.
7) Kita, K. et al.：Role of complex II in anaerobic respiration of the parasite mitochondria from Ascaris suum and *Plasmodium falciparum*. *Biochim. Biophys. Acta*, **1553**：123-139, 2002.
8) Ullmann, R. et al.：Transport of C(4)-dicarboxylates in Wolinella succinogenes. *J. Bacteriol.*, **182**：5757-5764, 2000.
9) Phang, J.M. et al.：The metabolism of proline, a stress substrate, modulates carcinogenic pathways. *Amino Acids*, **35**：681-690, 2008.
10) Droge, W.：Autophagy and aging-importance of amino acid levels. *Mech. Ageing Dev.*, **125**：161-168, 2004.
11) Mizushima, N. and Klionsky, D.J.：Protein turn-